

Passive fMRI mapping of language function for pediatric epilepsy surgical planning: validation using Wada, ECS, and FMAER

Ralph O. Suarez¹, Vahid Taimouri¹, Katrina Boyer³, Clemente Vega³, Alexander Rotenberg⁴, Joseph R. Madsen², Tobias Loddenkemper⁴, Frank Duffy⁴, Sanjay P. Prabhu¹, and Simon K. Warfield¹

Boston Children's Hospital, Harvard Medical School, Boston, USA

Departments of ¹Radiology, ²Neurosurgery, ³Neuropsychology, ⁴Neurology

Corresponding author: Ralph O. Suarez

Email: Ralph.Suarez@childrens.harvard.edu

Phone: 617-355-2755

Fax: 617-730-4644

1. INTRODUCTION

The mapping of language is important in pediatric patients who will undergo resection surgery near cortical regions essential for language function. However, due to young age, pediatric patients are typically unable to comply with complicated functional mapping protocols—particularly invasive clinical gold-standards, as well as non-invasive imagining techniques more easily used with adult

populations. A trend presently in the field promotes resection surgery to cure or prevent disease progression in increasingly younger epilepsy patients. This creates an urgent demand for reliable functional language mapping methods in characteristically incooperative patients, those often ineligible to undergo the invasive functional mapping gold-standards. In this article, we address this need by introducing functional magnetic resonance imaging (fMRI) methodologies for mapping of language in pediatric patients. Our approach evokes language activation without the need of overt compliance from the patient, and as such is designed for presurgical planning in pediatric patients.

The goal of brain resection is maximal removal of diseased tissue while at the same time minimizing potential damage to the eloquent brain systems. Resection surgery can raise the risk of damaging one or both language centers of the brain, resulting in permanent postsurgical language deficit (Duffau et al. 2009; Loisel et al. 2012; Matsuda et al. 2012). Determining the lateralization and localization of the essential language centers in relation to the surgical site therefore provides surgeons with a valuable tool for evaluating risk of postoperative morbidity associated with language deficit (Abou-Khalil et al. 2007; Sharan et al. 2010). Among the initial considerations in this evaluation is establishing the language dominance of the patient. Language dominance is of particular importance in patients for whom the planned surgical site is in the left cerebral hemisphere, as the vast majority of the population is left hemisphere dominant for language – on the order of 90% for the general healthy population (Wada and Rasmussen, 1960; Binder et al. 1996; Knecht et al. 2000). A planned resection in the same cerebral hemisphere as the patient's language dominance will consequently increase the risk of postsurgical language impairment. In such cases, a more precise localization of eloquent cortical regions is often determined by awake functional mapping in the operating room. The clinical gold-standards for determination of language lateralization and language localization are

the intracarotid sodium amobarbital procedure (Wada test) and direct electrocortical stimulation (ECS) mapping, respectively (Wada and Rasmussen, 1960; Ojemann et al. 1993). Functional MRI of language is a noninvasive alternative used with increasing frequency as a noninvasive alternative (Beers and Federico 2012; Garrett et al. 2012). Clinical fMRI language mapping has the potential for providing analogous language mapping measures to that of the clinical gold-standards noninvasively, and therefore is well suited for application in the youngest patient populations.

In previous work we demonstrated that an active fMRI language tasks, such as vocalized antonym-generation, produces lateralization and localization of cortical language processing highly congruent with gold-standards in adult epilepsy surgical patients (Suarez et al. 2009 and 2010). However, the mapping of language in pediatrics presents additional challenges. Children can be expected to have shorter attention spans to follow complicated cognitive tasks, and less tolerance for holding still during prolonged or complicated paradigms. The ideal pediatric fMRI paradigm therefore should be simple for the patient to perform and fast to acquire. In this study, we compare fMRI language mappings acquired using the active antonym-generation task we previously validated in adults (Suarez et al. 2008; Tie et al. 2009; Suarez et al. 2009), to a passive listening paradigm more ideally suited for application in pediatric clinical populations as it does not require any overt patient participation and can be acquired in approximately 7 minutes.

Given the clinically relevant information obtained from fMRI language maps in epilepsy surgical candidates, it is necessary to clearly define image-based indicators of map quality. We therefore defined a list of quality checks (QC) in order to evaluate the reliability of the language activation maps obtained for clinical applications. This novel approach defines a systematic protocol for

identifying, correcting, or if necessary, rejecting activation maps based on the following QC measures:

- Patient motion – quantitative assessment of head motion from translation and rotation during the full fMRI time series
- Functional overlay to structural underlay alignment – quantitative assessment of proper alignment between the functional map and the underlying anatomical reference frame (typically T1-weighted structural images)
- Behavioral-specific primary motor activation – confirmation of requisite primary motor cortex activation consistent with patient compliance for the behavioral task
- Stimulus-specific primary sensory activation – confirmation of requisite primary sensory cortex activation consistent with stimulus perception by the patient (primary auditory cortex or primary visual cortex, depending on the stimulus mode used)
- Language-specific activation – confirmation of activation in the putative language centers of the inferior frontal and temporoparietal cortices

These measures represent quantifiable features which while practical in nature are often overlooked or neglected in standard fMRI practices. In particular, the use of behavioral-specific and sensory-specific activations are often ignored, or actively eliminated by intricately designed fMRI subtraction schemes (Binder et al. 2008; Szenkovits et al. 2012; Stoppelman et al. 2013). However, we argue that if such non-language sensory-specific activation is not robustly apparent in the fMRI activation pattern, the diagnostic value of the language-specific activation pattern also should not be relied upon.

In this study, we initially perform a comparative study of active language fMRI (previously validated) against passive language fMRI (no yet validated); we recruited a healthy, right-handed control cohort of volunteers age-matched to a cohort of presurgical pediatric epilepsy patients. This control cohort was chosen as it can be expected to demonstrate typical language activation patterns—characterized by left-dominant activation of the putative language centers in the left inferior frontal and left temporoparietal regions, classically referred to as Broca’s and Wernicke’s areas, respectively (Broca et al. 1861; Wernicke et al. 1874). We test the hypothesis that our passive language fMRI task will activate both language centers of the brain similarly as the active task. We then validate the passive language fMRI findings in surgical patients by comparisons to the clinical gold-standards. Finally, we illustrate the use of our recommended methods in a challenging cohort of very young and sedated presurgical patients (mean age 7.5 years).

Pediatric temporal lobe epilepsy patients who undergo clinically-indicated Wada test and/or implantation of subdural electrodes with ECS mapping are a unique cohort with whom to validate language mappings done noninvasively by fMRI. The clinical gold-standard for lateralization of language is the Wada test, and ECS is the gold-standard for the localization of essential language regions. As such, results from these invasive modalities typically serve as the ground-truth for the evaluation of noninvasive fMRI results. In particular, validation of fMRI language lateralization is based on comparison against Wada testing in the same patient (Binder et al. 1996; Suarez et al. 2009), and validation of fMRI language localization is based on comparison against ECS functional mapping performed on the patient (Petrovich et al. 2007; Suarez et al. 2010). In addition, the frequency modulated auditory evoked response (FMAER) recorded from scalp electrodes has been previously shown to identify key aspects of language-level processing from auditory stimuli (Green

at al. 1979 and 1980; Stefanatos et al., 1989). More recently, we have recorded FMAER from intracranial implanted electrode grids to localize cortical function associated with language-level auditory processing (Duffy et al. 2013).

The goal of this study is to extend clinical fMRI mapping of cognitive function for epilepsy surgical applications in adults (Branco et al. 2006; Suarez et al. 2008, 2009, and 2010) to more challenging populations, and to demonstrate feasibility of performing reliable fMRI language mapping in presurgical pediatric epilepsy patients. We perform a validation study using a cohort of 15 surgical patients who undergo both preoperative language fMRI and invasive functional language mapping in the clinic. Finally, we present passive language fMRI results from an additional cohort of 6 patients who were too young to receive invasive mapping (mean age: 7.5 years), two of whom were sedated during scanning.

2. METHODS

2.1. Study participants and consent:

We recruited 25 right-handed volunteers (hand dominance determined by The Edinburgh Handedness Inventory, Oldfield RC 1971) with no history of neurologic disorders to participate in noninvasive MR imaging and language mapping, 14 females and 11 males mean age of 14.2 years (SD: 3.5 years).

The total patient cohort consisted of two populations. One patient cohort consisted of 15 pediatric epilepsy surgical patients, 8 females and 7 males mean age of 14.6 years (SD: 3.0 years), all of whom underwent clinically-indicated invasive testing to map language function as part of their clinical evaluation at Boston Children's Hospital (BCH). The second patient cohort consisted of younger patients, 4 female and 2 males, mean age of 7.5 years (SD: 1.8 years). All patients were diagnosed with pediatric onset epilepsy, and underwent comprehensive neuropsychological evaluation as part of the process for determining surgical candidacy: Verbal Comprehension Index (AVG: 92.9, SD: 25.1); Perceptual Reasoning Index (AVG: 97.8, SD: 13.8). Informed signed consent and institutional approval for medical records reviews was obtained in accordance with Institutional Review Board (IRB) regulations.

2.2. Imaging protocols:

All of the participants in our study, 46 in total (25 controls and 21 patients) attended MRI imaging to acquire high-resolution T1-weighted anatomical images and functional MRI imaging (3-Tesla Trio scanner, Siemens, Germany); 5 of the 15 patients also received computer tomography (CT) imaging (General Electric Medical Systems, USA) in order to localize indwelling cortical electrode strip and grid positions with respect to the surrounding brain anatomy.

We acquired high-resolution T1-weighted images using 3D Magnetization Prepared Rapid Acquisition Gradient Echo (MPRAGE). Typical imaging parameters consisted of: 24cm field-of-view (FOV), 1.0mm contiguous slice thickness, sagittal slices covering the entire head,

TR/TE=1410ms/2.27ms, matrix 256x256, TI=800 ms, and a flip angle=9-degrees; scan duration was approximately 7 min.

For 5 of the 15 patients, those who had intracranial electrodes implanted for seizure localization, CT scans of the head were acquired shortly after strip and grid implantation; CT imaging was carried out using a tube voltage of 125kV, and voxel size of $0.5 \times 0.5 \times 0.625 \text{mm}^3$, with FOV=500mm.

We compared two language paradigms designed to be administered in less than 7 minutes, and which use simple behavioral tasks easy to perform by pediatric subjects—vocalized antonym-generation presented in visual mode and passive story narrative paradigm presented in auditory mode. Functional MRI imaging was implemented in blood-oxygen-level-dependent (BOLD) acquisitions using a 32-channel head coil configured to accommodate MRI-compatible visual and auditory presentation equipment (Resonance Technology, Inc., USA). Typical scanning parameters consisted of: 24cm FOV; image matrix 128x128, between 3.0 – 4.0 mm thick contiguous axial slices in order to cover the entire brain; TR/TE=2500ms/31ms; and a flip angle=90-degrees.

Active language fMRI: visually presented, vocalized, antonym-generation task presented in a rapid, event-related fMRI paradigm consisting of presentation of antonym cue words (e.g., **UP**, **LEFT**, **OPEN**, etc) presented as black text on white background for 2 sec each with a pseudo-random inter-stimulus interval of 8 sec on average. Between each cue word, a fixation point was presented at center of the monitor; participants were asked to articulate a word having the opposite meaning as each of the cue words presented (e.g., **DOWN**, **RIGHT**, **CLOSE**, etc) without moving their head.

Visual stimulus was presented using MRI-compatible video goggles (Resonance Technology, Inc., USA). Total scan duration: 5.5 min with a TR of 2.5 sec.

Passive language fMRI: auditory presentation of a children's story narrative read by a female, monotone voice presented in a standard fMRI blocked design interleaving 40 sec intervals of passive listening to the story narrative contrasted with 40 sec intervals of silence. Participants were asked to listen to the sounds they hear holding their head still while fixated on the fixation point at center of the monitor. Auditory stimulus was presented using MRI-compatible headphones (Resonance Technology, Inc., USA). Total scan duration: 6.5 min with a TR of 2.5 sec.

BOLD contrasts, fMRI thresholds, and overlays: standard preprocessing of fMRI volumes was done including low band pass filtering, spatial smoothing with 8mm kernel, and rigid alignment of all fMRI BOLD time-series acquisition volumes (128 for antonym-generation task and 155 for passive story narrative task). Highly activated cortical regions were then identified in fMRI images by statistical parametric mapping (SPM5 Wellcome Laboratories, UK) based on the statistical correlation between BOLD signal fluctuations and the stimulus presentation paradigm used. We generated BOLD contrasts for antonym-generation compared to rest (silent viewing of fixation point), and for passive story narrative presentation compared to rest. Activation maxima in fMRI maps were identified after setting a threshold based on the uncorrected P statistic – all fMRI activation maps were thresholded at 0.05 or better, to avoid excessive false negatives in family-wise-error frequency rate; however, lateralization calculations were done independent of any threshold setting (Suarez et al, 2008 and 2009). Functional MRI activation maps were rigidly aligned,

resampled to high-resolution T1-weighted voxel dimensions, and overlaid onto T1-weighted anatomical volume.

2.3. fMRI QCs:

2.3.1. Participant Motion: quantitative assessment of patient motion was performed for each fMRI session acquired. This QC evaluates the amount of translations and rotations performed during standard rigid alignment of BOLD time-series volumes to the mean BOLD signal using rigid alignment. We define unacceptable amounts of x, y, z translations as those equal to or greater than twice the largest dimension of the fMRI image voxels, when occurring for more than one third of the full time series. That is, translations greater than 6.6 mm with respect to any Cartesian direction. Unacceptable degree of rotation was defined as rigid alignments greater than 1.0-degree with respect to any rotational axis. See Figure 1.

2.3.2. Functional overlay to structural underlay alignment: quantitative assessment of the alignment between fMRI functional overlay and anatomical T1-weighted underlay reference frames was performed on all acquisitions. This QC required confirmation of proper alignment between the mean BOLD volume and the anatomical T1-weighted underlay volume, see Figure 2. We used a standard rigid alignment algorithm based on mutual information in order to align the BOLD time series mean to the T1-weighted reference volume. We required accurate fMRI to anatomical volume

alignment precision to within the order of T1-weighted anatomical voxel size in each plane ($0.5 \times 0.5 \times 0.625 \text{mm}^3$). Any misalignment errors were by this means identified, and if necessary corrected. Often, alignment improvements were achieved by aligning the fMRI mean to skull-stripped versions of the T1-weighted anatomical reference using methods previously described (Grau et al. 2004; Weisenfeld and Warfield, 2009).

2.3.3. Behavioral-specific primary motor and sensory-specific primary visual activation:

antonym-generation fMRI activation maps were inspected in order to confirm requisite sensory-specific and motor-specific activation. This QC confirms robust, focal activation of the primary visual centers bilaterally in the occipital lobes consistent with sensory processing of visually presented antonym cue words. Additionally, as the task required vocalized responses, we inspected all activation maps to confirm robust, bilateral, focal activation of primary motor cortex consistent with articulation of the response words (often this activation was accompanied by activation of supplementary motor cortex in the midline). The presence of this activation pattern confirms the participant perceived the visual stimulus presented and consistently vocalized the antonym response words; in this way confirming successful visual stimulus delivery and participant compliance for the active task. See Figure 3. Absence of these activation patterns classified the fMRI map as unreliable and therefore was excluded from further analysis.

2.3.4. Sensory-specific primary auditory activation:

passive language fMRI activation maps were inspected in order to confirm sensory-specific activation from aurally presented story narrative. This QC required confirmation of robust, focal activation of the primary auditory cortex bilaterally in the

middle portion of the superior temporal gyrus consistent with proper auditory perception of the auditory stimulus. Absence of this sensory-specific activation pattern rendered the fMRI map unreliable and therefore was excluded from further analysis. See Figure 4.

2.3.5. Language-specific activation: all fMRI activation maps were then inspected in order to confirm robust, local activation maxima in regions of the brain consistent with the putative language centers of the: 1) inferior frontal gyrus (IFG), and 2) temporoparietal regions (TPG). This activation is typically lateralized favoring one cerebral hemisphere over the other, often the left (Wada and Rasmussen, 1960; Binder et al. 1996; Knecht et al. 2000), see Figure 5. The x, y, z coordinates of IFG and TPG local activation peaks were identified and recorded for localization validation.

2.4. Lateralization of language fMRI:

We quantified language activation asymmetry using an algorithm independent of fMRI threshold. We previously described this approach in detail (Branco et al. 2006; Suarez et al. 2008 and 2009). Briefly, a unique laterality index (LI) was calculated based on the T-squared weighted sums of the un-thresholded positive fMRI activation correlation values recorded within the two language-specific regions-of-interest (ROIs): 1) the IFG, and 2) the TPG regions. See Figure 5. This calculation yielded a unique LI value for each ROI in the range between -1.0 , 0.0 , and $+1.0$, where negative LI values indicate right-lateralized activation, positive LI values indicate left-lateralized activation, and absolute LI values less than or equal to 0.1 indicate no activation asymmetry (Suarez et al. 2008 and 2009).

2.5. Comparison of fMRI tasks in healthy controls:

We compared the previously validated vocalized antonym-generation language task (Suarez et al. 2008 and 2009) to passive language fMRI in the control cohort of 25 individuals, see Table 1. Subject and group region-specific LIs for IFG and TPG were calculated in order to evaluate language-specific activation asymmetry trends for the two task conditions. Each subject's LI were plotted and the mean LI for the group tabulated and compared across task conditions. Active and passive language fMRI paradigms were judged based on ability to activate the known language centers and demonstrate preponderance for left-dominant language processing in the control cohort.

2.6. Validation of fMRI in temporal lobe epilepsy patients:

The validation of passive language fMRI was carried out on patient cohort 1, made up of 15 pediatric-onset temporal lobe epilepsy surgical patients all of whom had some form of invasive mapping for comparisons against fMRI activation patterns. See Table 2. As part of their standard surgical workup, these patients underwent fMRI language mapping as well as clinically-indicated lateralization of language function by Wada testing and/or localization of eloquent language cortex by ECS. Five of these 15 patients additionally underwent recording of subdural FMAER evoked responses, which were used to validate auditory evoked activation by passive fMRI. Thirteen of these 15 patients had clinically-indicated language dominance determined by Wada testing, for comparison against fMRI LIs for IFG and TPG. Five of these 15 patients had ECS sites confirmed

for essential language function and were used to compare against fMRI language activation. Language localizations were assessed based on the Cartesian distance mismatch between positive electrode sites by found by ECS and fMRI activation peaks.

2.7. Testing of passive fMRI in cohort 2:

In a second patient cohort (cohort 2), we tested passive language fMRI in a challenging population of patients who because of their young age were not candidates for invasive functional mapping. Cohort 2 consisted of 6 patients (age 5, 8, or 9 years), two of who generally undergo MRI scanning under clinically-indicated sedation: patients p20 and p21; age 5 and 8 years. Please see Table 2. Passive language fMRI activation patterns in cohort 2 were used as compelling proof-of-concept in the most challenging pediatric population.

2.8. Neuropsychological measures:

Sixteen of twenty-one patients underwent recent neuropsychological evaluation as part of their standard presurgical workup. All measures were administered by a licensed clinical neuropsychologist or by a postdoctoral fellow in neuropsychology under the supervision of a licensed clinician. Intellectual functioning (VCI and PRI) were assessed using the Wechsler Intelligence Scale for Children-Fourth Edition.

2.9. Wada testing procedures:

Clinically-indicated intracarotid sodium amobarbital procedure (Wada) was conducted in 13 of 21 patients as part of the standard epilepsy surgery candidacy determination at BCH. The procedure involved administration of 100-150 mg of amobarbital to the presumed lesional hemisphere, followed by administration to the nonlesional hemisphere approximately 30 minutes later; neurobehavioral evaluation was administered immediately after each injection. Effects of medication were confirmed by contralateral hemiparesis and EEG slowing at the target hemisphere. A battery of language tests was completed including single-word comprehension, confrontation naming, repetition of phrases, and recitation of complex verbal sequences such as reciting months of the year in reverse order. Region-specific lateralization outcome was determined for receptive and expressive language functions separately for each patient.

2.10. Direct electrocortical stimulation mapping (ECS):

Clinically-indicated functional language mapping by direct electrocortical stimulation was performed in 5 of the 21 presurgical patients; ECS mapping was carried out utilizing electrode strips and grids previously implanted for standard phase II monitoring at BCH. The implanted electrodes consisted of stainless-steel or platinum-iridium alloy electrode discs 4mm in diameter arranged in grids of: 8×8, 8×4, or 8×2, or strips of: 8×1, 6×1, or 4×1, with an inter-electrode spacing of 10mm center-to-center (AdTech, Racine, USA). After implantation, strips and grids were sutured to the dural membrane. Patients p01, p02, p08, p11, and p12 received ECS functional mapping of language.

To map the regions essential to language by ECS, patients were awoken after craniotomy and asked to perform behavioral language tasks designed to test receptive and expressive language functions, including overt repetition of words, simple phrases, or sentences, and recitation of sequences such as reciting months of the year, or days of the week. While patients performed these behavioral tasks, brief electrical currents were systematically applied to the strip and grid electrodes using an IRES 600 CH electrical stimulator (Micromed, Italy; 50 Hz, 4e7 s, 1.5e10 mA). Intensity of the stimulations was adjusted for each patient in order to maximize the stimulation effect while at the same time minimizing the occurrence of after-discharges. Electrode stimulation sites were considered positive for essential language function if disruption of the behavioral task was consistently observed upon two or three separate stimulations; the unique number indentifying that electrode site was recorded. Stimulations that were accompanied by after-discharges were screened for the occurrence of spread to other electrodes and when this occurred the respective stimulation was excluded from further analysis. We measured the Cartesian distance between the ECS electrodes confirmed for language function and the localization of peak fMRI TPG activation for language processing. Note that cortical stimulation sites in each patient were by necessity limited to the specific electrode coverage clinically-indicated in each patient for the purpose of epileptogenic foci localization and not necessarily for comprehensive functional mapping.

2.11. Frequency modulated auditory evoked responses (FMAER):

Subdural FMAER responses were recorded in 5 of the 15 patients in cohort 1. The FMAER procedures used were described in detail in a previous publication (Duffy et al. 2013). Briefly, we administered aurally presented stimulus consisting of a carrier sine wave at 1000 Hz frequency modulated by a slower 10 Hz sine wave, causing the frequency of the carrier wave to deviate between 960 and 1060 Hz at the 10 Hz rate and thus producing a frequency modulation warbling tone. Next, a 10 Hz sine wave was amplitude modulated by a slower 4 Hz sine wave such that the warbling was sinusoidally turned on and off at 4 Hz rate. Each stimulus onset was used to trigger separate epochs used for signal averaging and generation of the averaged evoked response. Typically 300–1000 msec trigger pulses were averaged over an epoch duration of 1000 msec (Green et al. 1979 and 1980). Data were recorded directly from the cortex utilizing indwelling electrodes. Recordings that contained continual or frequent seizure discharges or electrodes that had not been placed near or over the temporal regions were not included in the analysis. Signal averaging was performed using BESA GmbH (v6.0, Germany). Only the electrode(s) demonstrating the maximal evoked responses following 4 Hz FMAER stimulus were recorded for our analysis; we measured the Cartesian distance between the uniquely numbered electrodes and the localization of peak fMRI primary auditory activation for language stimuli.

2.12. Preparation of 3D surfaces for electrode grid and fMRI map co-registrations:

In order to produce co-registrations and 3D models of ECS, FMAER, and fMRI mapping results for comparative study in the same patient, we utilized an alignment algorithm we previously described in detail (Taimouri et al. 2013). Briefly, we created a patient-specific 3D geometric model of the cortical brain surface by means of automatic segmentation of the T1-weighted anatomical images. The co-registration of T1-weighted anatomical volumes and CT images was achieved by mutual information rigid alignment. We then projected the grid electrodes onto the cortical surface in the perpendicular direction, that is, normal to the plastic sheet on which the electrodes were mounted. A unique normal vector was determined for the strip electrodes by minimizing the sum squared distances between electrodes and the plane crossing all of the strip electrodes. Lastly, we colored the 3D brain surface by fMRI activation maps in order to measure the Cartesian distance between positive electrode localization and local fMRI maxima. See Figure 7.

3. RESULTS

3.1. Comparison of fMRI tasks:

Both of the fMRI language tasks we tested in the control cohort demonstrated robust activation consistent with the expressive language region (IFG) and the receptive language region (TPG) in all

of the subject scans with satisfactory QCs (38 out of 50): 17 active language fMRI and 21 passive language fMRI.

In the control cohort, the active task demonstrated 94% incidence of left-lateralized IFG activation (mean LI: +0.38), and 74% incidence of left-lateralized TPG activation (mean LI: +0.15), compared to the passive task which demonstrated 67% incidence of left-lateralized IFG activation (mean LI: +0.24), and 86% incidence of left-lateralized TPG (mean LI: +0.45). These comparisons were summarized in Table 3 and Figure 6.

3.2. Validation of passive language fMRI:

Patient cohort 1 received passive language fMRI and invasive functional mapping by Wada testing and/or ECS. Two of the fMRI scans were re-acquired due to lack primary auditory activation in the first session (we suspected poor or no audio stimulus being delivered to the patient as a result of user error in the first attempt—the patient failed to report the problem). Patient p04 did not demonstrate the expected bilateral primary auditory activation (only observed in the left side), however, the lack of right activation was attributed to the presence of large lesion encompassing the primary auditory cortex of that side of the brain and therefore that fMRI scan was not repeated in that case. All of the fMRI scans acquired in the patient cohort with satisfactory QCs (15 of 15, after 2 scans were redone) demonstrated local fMRI activation peaks in IFG and TPG consistent with language-specific activation.

3.3. Validation of passive language fMRI lateralization:

Language lateralization by fMRI in the TPG ROI agreed with invasive clinical testing for receptive language dominance (Wada testing and ECS mapping) in 11 of 15 patients. Generally when fMRI was compared against these reference standards, we observed 80% congruency in TPG language activation, and 73% congruency in IFG activation. See Table 4.

The fMRI language lateralization of IFG agreed with Wada test language dominance for expressive language processing in 9 of 13 patients (70% fMRI to Wada test congruency); fMRI TPG lateralization agreed with Wada test for receptive language dominance in 10 of 13 patients (77% fMRI to Wada test congruency). Of 5 patients who received ECS language mapping, 4 showed dominant TPG activation by fMRI in the same cerebral hemisphere as essential receptive language processing localized by ECS (80% fMRI to ECS congruency).

3.4. Validation of fMRI localization:

In patient cohort 1, 5 of 15 patients received both ECS language mapping and FMAER localization. In the comparison between FMAER localizations and primary auditory activation from passive language fMRI, the mean distance mismatch observed was 14.4mm (SD: 5.7mm). In the comparison

between ECS language localizations and TPG language activation from passive language fMRI only 2 of the 5 patients (p01 and p02) had sufficient electrode coverage over the TPG activation region and as a result the distance mismatch could not be confirmed in those cases. In patient p01, TPG activation by fMRI localized over 50mm away from the nearest electrode. In patient p02, TPG activation localized to the right hemisphere, where there was no electrode coverage. With p01 and p02 results excluded, the mean distance mismatch between receptive language ECS electrodes and fMRI TPG activation was 9.2mm (SD: 2.6mm). These findings are summarized in Table 5 and Figure 7.

3.5. Testing of passive fMRI in cohort 2:

For 6 of 6 patients in cohort 2, we recorded robust bilateral fMRI activation of primary auditory cortex consistent with normal perception of the auditory narrative stimulus presented. In 6 of 6 patients in cohort 2 we detected lateralized activation consistent with typical left-lateralized processing of the putative temporoparietal language center; two of these patients (p17 and p20) demonstrated lateralized activation consistent with typical left-lateralized processing of the putative frontal language center. Patients p20 and p21 were sedated during passive language fMRI recording. See Figure 8.

4. DISCUSSION

In this study we defined, validated, and tested passive language fMRI imaging protocols which do not require any participation from the patient and are designed for reliable application in pediatric epilepsy applications.

We initially compared two fMRI language mapping paradigms: a previously validated protocol for adults (Suarez et al. 2008 and 2009) which is active in nature (vocalized antonym-generation); and passive listening to a story narrative. Group-level analysis demonstrated that both tasks produced consistent activation in the two main language centers. We found that the active task more robustly activated the expressive language region (IFG) compared to the receptive language region (TPG), while the passive task more robustly activated TPG compared to IFG. Additionally, more left-lateralized activation was observed in IFG (LI = +0.38) compared to TPG (LI = +0.15) using the active task, whereas more left-lateralized activation was observed in TPG (LI = +0.45) compared to IFG (LI = +0.24) using the passive task.

We then validated the passive language fMRI in cohort 1, made up of 15 presurgical patients with invasive functional mapping results. The validation approach compared language dominance by Wada testing and ECS, against functional lateralization by fMRI; FMAER peak response localizations were compared against auditory-specific activation by fMRI; and ECS language localizations against language-specific TPG activation by fMRI. We confirmed strong fMRI congruency to the invasive clinical procedures: 80% congruency with respect to TPG activation, and 73% congruency with respect to IFG activation. In the comparison between fMRI and FMAER for

the 5 patients tested, we found a mean FMAER to fMRI mismatch distance of only 14.4mm. In the comparison between ECS and TPG activation in the 3 patients tested with sufficient electrode coverage, we observed a mean ECS to fMRI mismatch distance of only 9.2mm.

Lastly, we tested the recommended passive language fMRI and QC protocols in a challenging cohort of very young patients, cohort 2, two of who were sedated during scanning. Reliability evaluation of these fMRI maps was based on our recommended quality checks (QC)—primarily on detection of expected sensory-specific primary auditory activation patterns, and detection of lateralized activation patterns in the putative language regions consistent with language-specific cortical processing. We confirmed reliable activation patterns from passive language fMRI in 6 of 6 patients in this challenging cohort.

There is a recent trend which advocates increased indication for surgical intervention in younger epilepsy patients than was true in the past. It is now understood that in most cases, early and minimally invasive surgery is essential for successful management of epilepsy progression in children (Holthausen et al. 2013; Glauser and Loddenkemper, 2013). Accordingly, children who in the past were excluded from epilepsy surgery, for example due to early onset age or presentation of multiple lesions, are now in greater numbers becoming surgical candidates (Beier and Rutka 2013; Holthausen et al. 2013). While the gradually widening spectrum of indications for surgery in children is shown effective for preventing later-stage development of more catastrophic disease manifestations (Holthausen et al. 2013), it places greater than before emphasis on reliable presurgical language mapping in increasingly younger patients. Because passive language fMRI can be administered quickly and simply (7min scan which does not require any behavioral participation

from the patient) and is therefore ideal for use with younger patients who may not be expected to comply with the more complicated behaviorally active tasks.

Localization of neurophysiological activity in the brain is most reliably mapped by direct mapping techniques applied subdurally to the cortical surface, such as ECS (Ojemann et al. 1993). Intracranial electrode strips and grids implanted for invasive monitoring in presurgical epilepsy patients hence offers a unique opportunity to perform activation studies using the same averaged evoked potential paradigms used for decades with scalp electroencephalography and magnetoencephalography (Green et al. 1979 and 1980; Reite et al. 1978; Stefanatos et al., 1989). The frequency modulated auditory evoked response (FMAER) techniques used in this study localize sensory-specific activation of the auditory cortex which in addition to processing simple sensory perception of the stimulus also holds promise as a proxy for language-level processing from the FM stimulus presented (Duffy et al. 2013). In this study, we found that sensory-specific fMRI activation produced by auditory presentation of a story narrative agreed to within 15mm with the electrodes of peak FMAER responses. This close proximity provides compelling validation for fMRI localization of auditory-level processing of the language-specific stimulus in the passive language paradigm.

Invasive functional mapping of language processing by ECS, in contrast to the evoked FMAER responses, is a deactivation technique which aims to identify and localize the cortical sites which are essential for language function (Ojemann et al. 1993). Application of electric currents to the implanted electrodes in effect produces a temporary lesion which momentarily ceases cortical function at the application volume. By electrically deactivating the cortical sites which if damaged during resection cause similar postsurgical language deficits, the ECS technique is currently the

reference standard for localizing essential language in the brain. However, ECS functional language mapping is an invasive procedure requiring adequate electrode coverage over the essential language regions, awake surgery, and strict patient task compliance intra-operatively after craniotomy. For these reasons, functional language mapping by ECS is extremely limited or not feasible in very young or in compliant patients. We found that in most cases, receptive language activation by fMRI acquired passively agreed with ECS localization of essential receptive language function to within 10mm.

The novel set of QCs we recommend for clinical fMRI language mappings were designed to rule out many common errors which if not identified (and if possible corrected) would render the fMRI activation maps unreliable, but which to our knowledge have never been used to systematically classify fMRI maps as unreliable. When assessing fMRI language maps, we recommend close attention to non-language activation patterns, such as sensory or motor activation which while not directly associated with language processing are nevertheless required features consistent successful application of a particular fMRI language protocol. For example, visual words or auditory presentation of a story narrative by necessity require initially the sensory-specific perception of the stimulus by the patient (e.g., primary visual cortex, or primary auditory cortex, depending on the stimulus mode used). Therefore, the absence of this sensory-specific activation indicates that the resulting activation map is inconsistent with the fMRI paradigm and should not be relied upon to correctly delineate language-specific activation in the clinic. In prior studies by others, subtraction schemes have been proposed in order to eliminate non-language activation, typically by carefully defined baseline conditions and subtraction methodologies (Binder et al. 2008; Szenkovits et al. 2012; Stoppelman et al. 2013), or precisely timed MRI scanner sampling schemes (Birn et al. 1999;

Preibisch et al. 2003). However, it is not clear how to define the most appropriate choice of baseline condition, which eliminates all of the non-language activation while not at all impacting language-specific activation patterns. It is also not clear that non-language activation is irrelevant for the analysis of language-specific activation patterns. We additionally point out that while a myriad of factors could potentially lead to alignment errors when creating fMRI map overlays, often these alignment errors are not detected or are ignored; thereby introducing localization errors in activation maps.

By applying the recommend QCs systematically to the fMRI activation maps in our control population, we were able to determine that while overt antonym-generation task can more robustly activate frontal language processing in IFG, it also has a higher likelihood of poor task compliance or becoming contaminated by excessive patient motion compared to the passive narrative task. This indicates that in most pediatric temporal lobe epilepsy surgical candidates, the fMRI mapping of essential language can proceed with passive language fMRI. This protocol similarly holds strong promise for routine use with sleeping, sedated, or unconscious patients in whom language mapping would otherwise not be possible. We presented compelling evidence that our recommended fMRI language mapping protocols will noninvasively produce language maps which are equivalent with the invasive clinical procedures.

5. CONCLUSIONS

We have shown that our recommended passive language fMRI paradigm can be applied for reliable determination of language dominance and language functional localization in children as young as 5-9 years of age, including patients who are sedated. As such, the fMRI protocols we present effectively meet an increasing demand for reliable noninvasive functional mapping of language in very young presurgical epilepsy patients.

ACKNOWLEDGEMENTS

This research was funded in part by US Department of Defense Award: MS120015, National Multiple Sclerosis Society Pilot Grant: PP1625, and National Institutes of Health: R42 MH086984.

REFERENCES

Abou-Khalil B. An update on determination of language dominance in screening for epilepsy surgery: the Wada test and newer noninvasive alternatives. *Epilepsia*. 2007 Mar;48(3):442-55. Epub 2007 Feb 21. Review. PubMed PMID: 17319925.

Beers CA, Federico P. Functional MRI applications in epilepsy surgery. *Can J Neurol Sci*. 2012 May;39(3):271-85. Review. PubMed PMID: 22547506.

Beier AD, Rutka JT. Hemispherectomy: historical review and recent technical advances. *Neurosurg Focus*. 2013 Jun;34(6):E11. doi: 10.3171/2013.3.FOCUS1341. PubMed PMID: 23724835.

Birn, R. M., Cox, R. W., & Bandettini, P. A. (2004). Experimental designs and processing strategies for fMRI studies involving overt verbal responses. *Neuroimage*, 23(3), 1046–58 (Nov).

Binder JR, Swanson SJ, Hammeke TA, Sabsevitz DS. A comparison of five fMRI protocols for mapping speech comprehension systems. *Epilepsia*. 2008 Dec;49(12):1980-97. doi: 10.1111/j.1528-1167.2008.01683.x. Epub 2008 May 29. PubMed PMID: 18513352; PubMed Central PMCID: PMC2645716.

Binder JR, Swanson SJ, Hammeke TA, Morris GL, Mueller WM, Fischer M, Benbadis S, Frost JA, Rao SM, Houghton VM. Determination of language dominance using functional MRI: a comparison with the Wada test. *Neurology*. 1996 Apr;46(4):978–984.

Branco DM, Suarez RO, Whalen S, O'Shea JP, Nelson AP, da Costa JC, Golby AJ. Functional MRI of memory in the hippocampus: Laterality indices may be more meaningful if calculated from whole voxel distributions. *Neuroimage*. 2006 Aug 15;32(2):592-602. Epub 2006 Jun 13. PubMed PMID: 16777435.

Broca PP. Perte de la parole ramolissement chronique et destruction partielle du lobe antérieur gauche de cerveau. *Bulletins de la Société d'anthropologie de Paris*. 1861;2:235–238.

Duffau H, Moritz-Gasser S, Gatignol P. Functional outcome after language mapping for insular World Health Organization Grade II gliomas in the dominant hemisphere: experience with 24 patients. *Neurosurg Focus*. 2009 Aug;27(2):E7. doi: 10.3171/2009.5.FOCUS0938. PubMed PMID: 19645563.

Duffy FH, Eksioglu YZ, Rotenberg A, Madsen JR, Shankardass A, Als H. The frequency modulated auditory evoked response (FMAER), a technical advance for study of childhood language disorders: cortical source localization and selected case studies. *BMC Neurol*. 2013 Jan 25;13:12. doi: 10.1186/1471-2377-13-12. PubMed PMID: 23351174; PubMed Central PMCID: PMC3582442.

Garrett MC, Pouratian N, Liau LM. Use of language mapping to aid in resection of gliomas in eloquent brain regions. *Neurosurg Clin N Am*. 2012 Jul;23(3):497-506. doi: 10.1016/j.nec.2012.05.003. Review. PubMed PMID: 22748661; PubMed Central PMCID: PMC3618998.

Grau V, Mewes AU, Alcaniz M, Kikinis R, Warfield SK. Improved watershed transform for medical image segmentation using prior information. *IEEE transactions on medical imaging*. 2004;23:447–458.

Green GGR, Kay RH, Rees A. Responses evoked by frequency-modulated sounds recorded from the human scalp. *J Physiol*. 1979;296:21–22P. [PubMed]

Green GGR, Rees A, Stefanatos GA. A method for recording evoked responses to frequency modulated sounds in man. *J Physiol*. 1980;307:10p.

Glauser TA, Loddenkemper T. Management of childhood epilepsy. *Continuum (Minneapolis)*. 2013 Jun;19(3 Epilepsy):656-81. doi: 10.1212/01.CON.0000431381.29308.85. PubMed PMID: 23739103.

Holodny AI, Schulder M, Ybasco A, Liu WC. Translocation of Broca's area to the contralateral hemisphere as the result of the growth of a left inferior frontal glioma. *J Comput Assist Tomogr*. 2002 Nov-Dec;26(6):941-3. PubMed PMID: 12488739

Holthausen H, Pieper T, Kudernatsch M. Towards early diagnosis and treatment to save children from catastrophic epilepsy - Focus on epilepsy surgery. *Brain Dev.* 2013 Jun 20. doi:pii: S0387-7604(13)00166-6. 10.1016/j.braindev.2013.05.003. [Epub ahead of print] PubMed PMID: 23791480.

Knecht S, Dräger B, Deppe M, Bobe L, Lohmann H, Flöel A, Ringelstein EB, Henningsen H. Handedness and hemispheric language dominance in healthy humans. *Brain.* 2000 Dec;123 Pt 12:2512-8. PubMed PMID: 11099452.

Loiselle M, Rouleau I, Nguyen DK, Dubeau F, Macoir J, Whatmough C, Lepore F, Joubert S. Comprehension of concrete and abstract words in patients with selective anterior temporal lobe resection and in patients with selective amygdalo-hippocampectomy. *Neuropsychologia.* 2012 Apr;50(5):630-9. doi: 10.1016/j.neuropsychologia.2011.12.023. Epub 2012 Jan 8. PubMed PMID: 22245005.

Matsuda R, Coello AF, De Benedictis A, Martinoni M, Duffau H. Awake mapping for resection of cavernous angioma and surrounding gliosis in the left dominant hemisphere: surgical technique and functional results: clinical article. *J Neurosurg.* 2012 Dec;117(6):1076-81. doi: 10.3171/2012.9.JNS12662. Epub 2012 Oct 5. PubMed PMID: 23039148.

Oldfield RC. The assessment and analysis of handedness: the Edinburgh inventory. *Neuropsychologia.* 1971 Mar;9(1):97-113

Ojemann GA. Functional mapping of cortical language areas in adults. Intraoperative approaches. *Advances in Neurology*. 1993;63:155–163.

Petrovich Brennan NM, Whalen S, de Moraes Branco D, O'shea JP, Norton IH, Golby AJ. Object naming is a more sensitive measure of speech localization than number counting: Converging evidence from direct cortical stimulation and fMRI. *Neuroimage*. 2007;37 Suppl 1:S100–S108.

Preibisch,C.,Raab,P.,Neumann,K.,Euler,H.A.,vonGudenberg,A.W.,Gall, V., et al. (2003). Event related fMRI for the suppression of speech-associated artifacts in stuttering. *Neuroimage*,19(3), 1076–1084 (Jul).

Reite M, Edrich J, Zimmerman JT, Zimmerman JE. Human magnetic auditory evoked fields. *Electroencephalogr Clin Neurophysiol*. 1978 Jul;45(1):114-7. PubMed PMID: 78814.

Sharan A, Ooi YC, Langfitt J, Sperling MR. Intracarotid amobarbital procedure for epilepsy surgery. *Epilepsy Behav*. 2011 Feb;20(2):209-13. doi: 10.1016/j.yebeh.2010.11.013. Epub 2010 Dec 28. Review. PubMed PMID: 21190900.

Stefanatos GA, Green GGR, Ratcliff GG. Neurophysiological evidence of auditory channel anomalies in developmental dysphasia. *Arch Neurol*. 1989;46(August):871–875.

Stoppelman N, Harpaz T, Ben-Shachar M. Do not throw out the baby with the bath water: choosing an effective baseline for a functional localizer of speech processing. *Brain Behav*. 2013

May;3(3):211-22. doi: 10.1002/brb3.129. Epub 2013 Feb 17. PubMed PMID: 23785653; PubMed Central PMCID: PMC3683281.

Suarez RO, Whalen S, O'Shea JP, and Golby AJ. A Surgical Planning Method for Functional MRI Assessment of Language Dominance: Influences from Threshold, Region-of-Interest, and Stimulus Mode. *Brain Imaging and Behavior*. 2008; 2(2):59-73.

Suarez RO, Whalen S, Nelson AP, Tie Y, Meadows ME, Radmanesh A, Golby AJ. Threshold-independent functional MRI determination of language dominance: a validation study against clinical gold standards. *Epilepsy Behav*. 2009 Oct;16(2):288-97. doi: 10.1016/j.yebeh.2009.07.034. Epub 2009 Sep 4. PubMed PMID: 19733509; PubMed Central PMCID: PMC2758322.

Suarez RO, Golby A, Whalen S, Sato S, Theodore WH, Kufta CV, Devinsky O, Balish M, Bromfield EB. Contributions to singing ability by the posterior portion of the superior temporal gyrus of the non-language-dominant hemisphere: first evidence from subdural cortical stimulation, Wada testing, and fMRI. *Cortex*. 2010 Mar;46(3):343-53. doi: 10.1016/j.cortex.2009.04.010. Epub 2009 May 18. PubMed PMID: 19570530; PubMed Central PMCID: PMC2821975.

Szenkovits G, Peelle JE, Norris D, Davis MH. Individual differences in premotor and motor recruitment during speech perception. *Neuropsychologia*. 2012 Jun;50(7):1380-92. doi: 10.1016/j.neuropsychologia.2012.02.023. Epub 2012 Apr 12. PubMed PMID: 22521874.

Taimouri V, Akhondi-Asl A, Tomas-Fernandez X, Peters JM, Prabhu SP, Poduri A, Takeoka M, Loddenkemper T, Bergin AM, Harini C, Madsen JR, Warfield SK. Electrode localization for planning surgical resection of the epileptogenic zone in pediatric epilepsy. *Int J Comput Assist Radiol Surg*. 2013 Jun 23. [Epub ahead of print] PubMed PMID: 23793723.

Tie Y, Suarez RO, Whalen S, Radmanesh A, Norton IH, Golby AJ. Comparison of blocked and event-related fMRI designs for pre-surgical language mapping. *Neuroimage*. 2009 Aug;47 Suppl 2:T107-15. PubMed PMID: 19101639; PubMed Central PMCID: PMC3036974.

Wada J, Rasmussen T. Intracarotid injection of sodium amytal for the lateralization of cerebral speech dominance. *Journal of Neurosurgery*. 1960;17:266–282.

Weisenfeld NI, Warfield SK. Automatic segmentation of newborn brain MRI. *Neuroimage*. 2009 Aug 15;47(2):564–72.

Wernicke K. *Der aphasische Symptomencomplex. Eine psychologische Studie auf anatomischer Basis*. Breslau M. Crohn und Weigert; 1874.

TABLES

subject	sex	age	handedness
c01	M	11	+100
c02	M	8	+90
c03	F	16	+100
c04	F	10	+70
c05	M	11	+85
c06	M	10	+100
c07	M	17	+100
c08	F	8	+100
c09	F	18	+85
c10	M	16	+60
c11	F	17	+100
c12	F	16	+85
c13	M	17	+75
c14	F	17	+90
c15	F	17	+100
c16	M	16	+70
c17	F	11	+90
c18	F	12	+100
c19	F	9	+85
c20	F	16	+90
c21	M	12	+100
c22	M	16	+85
c23	F	15	+100
c24	F	19	+90
c25	M	19	+100
mean age (years):		14.2	

Table 1: *Healthy control cohort consisting of 25 volunteers age-matched and sex-matched to pediatric epilepsy surgical patients, all strong right-handers by the Edinburgh Handedness Inventory (Oldfield 1971).*

patient	sex	age	handedness	age at onset	VCI IQ	PRI IQ	epileptic localization
p01	M	16	R	12	53	70	left temporal
p02	M	17	R	7	-	-	left temporal/frontal/parietal
p03	F	17	R	13	149	115	left temporal
p04	M	16	R	9	116	119	right posterior quadrant
p05	F	13	L	6	93	106	left temporal
p06	M	10	L	1	71	88	left hemisphere
p07	F	19	R	6	72	86	right mesial temporal
p08	F	16	R	13	108	98	left temporal
p09	M	17	R	15	100	88	left temporal
p10	F	12	L	0	75	102	left frontotemporal
p11	F	13	R	3	-	-	left temporal
p12	M	12	L	5	-	-	left mesial temporal
p13	M	15	R	4	102	110	left temporal/frontal
p14	F	17	R	8	87	92	left temporal
p15	F	9	R	9	89	100	left temporal
mean age (years):		14.6		7.4			

Table 2: *Demographics and description of pediatric epilepsy patient cohorts; Verbal Comprehension Index (VCI) and Perceptual Reasoning Index (PRI) are shown. Data not shown were not available in those patients. Shown are the two patient cohorts used in the study, including their etiology and pathology data if available.*

subject	active task		passive task	
	IFG	TPG	IFG	TPG
c01	L	L	L	L
c02	L	L	L	L
c03	L	L	L	L
c04	-	-	R	L
c05	L	L	L	L
c06	L	L	L	L
c07	-	-	R	R
c08	-	-	R	L
c09	L	R	R	R
c10	R	R	-	-
c11	L	Bilateral	L	L
c12	L	R	R	L
c13	L	L	L	L
c14	L	R	L	L
c15	L	L	L	L
c16	L	L	L	L
c17	-	-	R	L
c18	L	L	R	L
c19	L	L	L	L
c20	-	-	-	-
c21	L	Bilateral	L	L
c24	L	L	L	Bilateral
c25	-	-	L	L
mean LI value:	+0.38	+0.15	+0.24	+0.45

TABLE 3: Control cohort language lateralization by fMRI using activate and passive fMRI tasks. Listed are group mean lateralization indices (LI) in the inferior frontal (IFG) and temporoparietal (TPG) language regions.

Positive LI indicate left (L) lateralization; (-) denotes omitted scans.

patient	Wada lateralization		ECS	fMRI lateralization	
	expressive	receptive		IFG	TPG
p01	L	L	Left TPG	L	L
p02	L	Bilateral	Left TPG	R	R
p03	L	L	-	L	R
p04	L	L	-	R	L
p05	Bilateral	Bilateral	-	L	R
p06	R	R	-	R	R
p07	L	L	-	R	L
p08	L	L	Left TPG	L	L
p09	L	L	-	L	L
p10	R	R	-	R	R
p11	-	-	Left TPG	R	L
p12	-	-	Left TPG	L	L
p13	Bilateral	L	-	Bilateral	L
p14	L	L	-	L	L
p15	L	L	-	L	L
cases congruent with clinical standards:				11/15 (73%)	12/15 (80%)

Table 4: Congruency between region-specific language lateralization by invasive clinical standards compared to fMRI. Shown are left, right (L, R), or bilateral expressive and receptive language dominance as determined by Wada testing; hemispherical localization of receptive language function as determined by direct electrocortical stimulation mapping (ECS); and language lateralization of the inferior frontal (IFG) and temporoparietal (TPG) language regions as determined by passive language fMRI. Bold lettering denotes instances of fMRI incongruity with the clinical reference standards.

patient	mismatch distance (mm)	
	FMAER - auditory fMRI	ECS - language fMRI
p01	13.3	> 50.0*
p02	22.3	> 50.0*
p08	10.6	12.1
p11	8.1	7.3
p12	17.6	8.1
mean (mm):	14.4	9.2

Table 5: *The cortical Cartesian distance mismatch between FMAER and primary auditory activation from passive language fMRI (FMAER – auditory fMRI), and between ECS language sites and TPG activation by passive language fMRI (ECS – language fMRI). Cases which did not have sufficient electrode coverage in regions identified as dominant for receptive language by fMRI are denoted with (*) and were excluded from the calculation of mean value.*

FIGURES

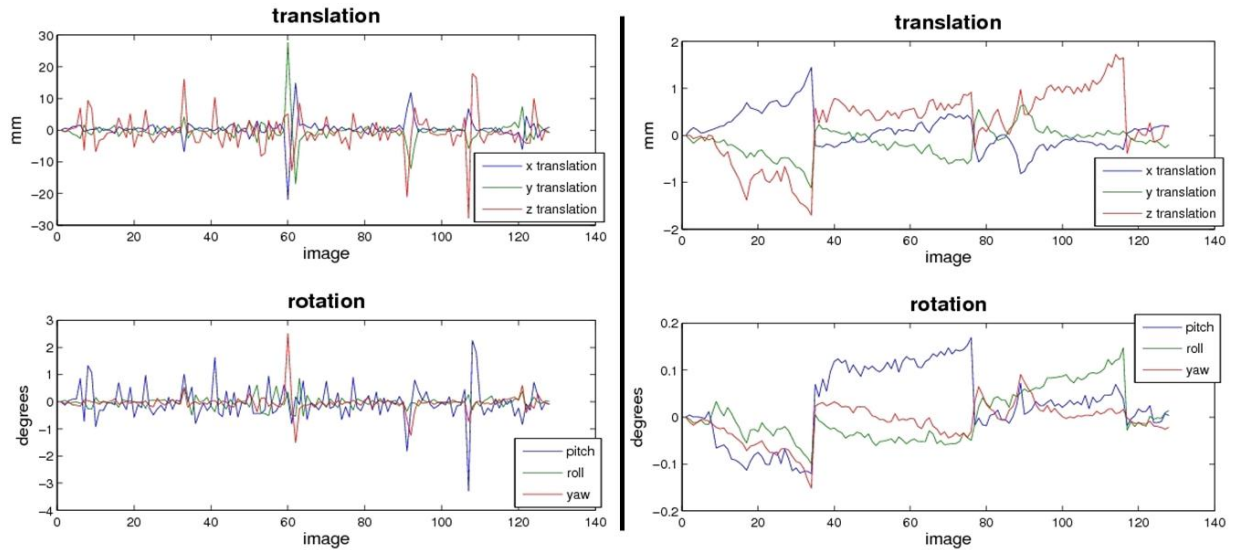


Figure 1: Motion parameters from SPM5 rigid alignments of fMRI time-series volumes and the BOLD mean, plotted as a function of each volume, top panels show x, y, z translations and bottom panels show pitch, roll, and yaw rotations. Left and right panels depict similar data for two representative subjects, left panel shows a scan with unaccepted amount of subject motion, right panel shows a representative scan with satisfactory amount of motion.

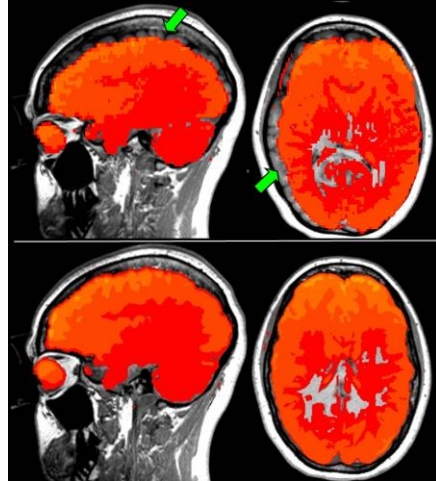


Figure 2: *Quantitative assessment of functional overlay to anatomical underlay alignment.*

Top panel depicts a representative subject scan illustrating poor alignment – note unacceptable alignment errors visible in the sagittal and axial planes (green arrows). Conversely, the bottom panel illustrates a representative example depicting proper alignment.

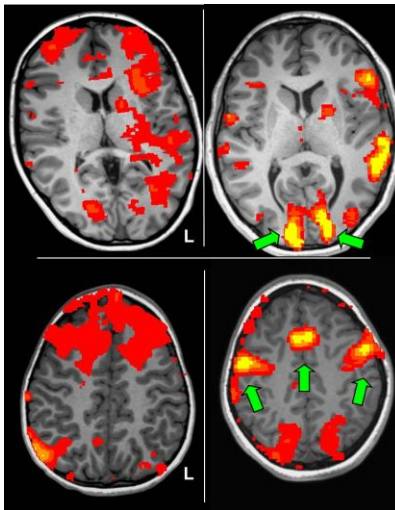


Figure 3: *Illustration of quality checks to confirm expected sensory-specific (top panels) and motor-specific (bottom panels) fMRI activation patterns from the active language task.*

A representative participant scan showing an unacceptable absence of robust, bilateral

activation of primary visual cortex is shown in the top left panel; conversely, the top right panel shows a representative scan with green arrows highlighting the expected activation pattern consistent with proper sensory perception of the visual cue words. The bottom left panel shows a scan with unacceptable absence of robust, bilateral activation of primary motor cortex; conversely, the bottom right panel shows an activation pattern consistent with articulation of antonym response words and thus compliance for the active task.

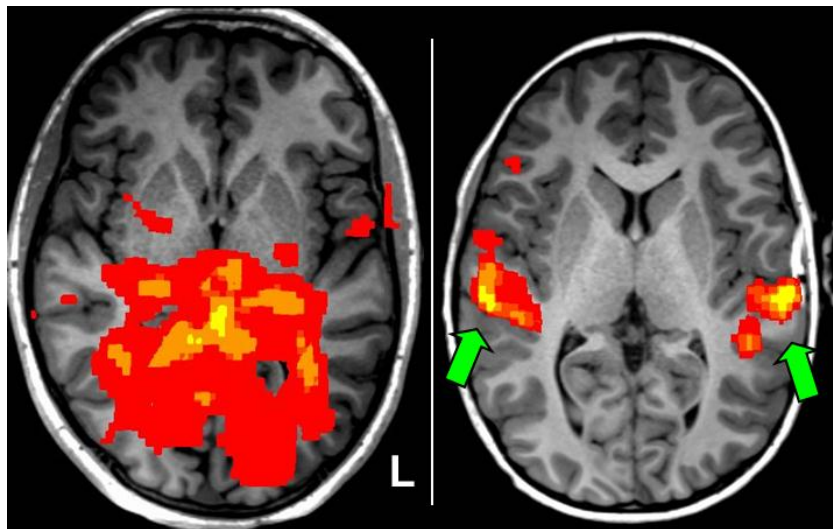


Figure 4: Illustration of quality check to confirm the expected sensory-specific fMRI activation pattern from passive listening to story narrative language task. A representative participant scan showing unacceptable absence of robust, bilateral activation of primary auditory cortex is shown in the left panel; conversely, the right panel shows a representative scan confirming robust, bilateral activation of primary auditory cortex (green arrows) consistent with proper sensory perception of the auditory stimulus.

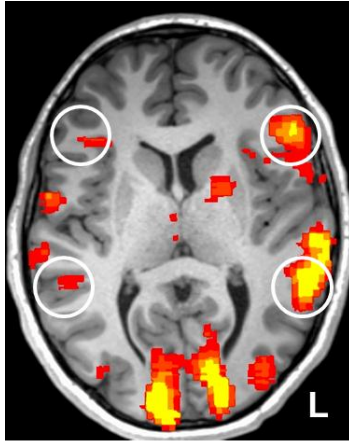


Figure 5: A representative fMRI language activation map ($p < 0.001$, uncorrected) from the visually presented antonym-generation task, note the expected language-specific activation peaks in the putative language centers of the inferior frontal gyrus and temporoparietal regions (white circles). Note the clear activation asymmetry across the cerebral hemispheres, in this case denoting typically left-lateralized language for this participant.

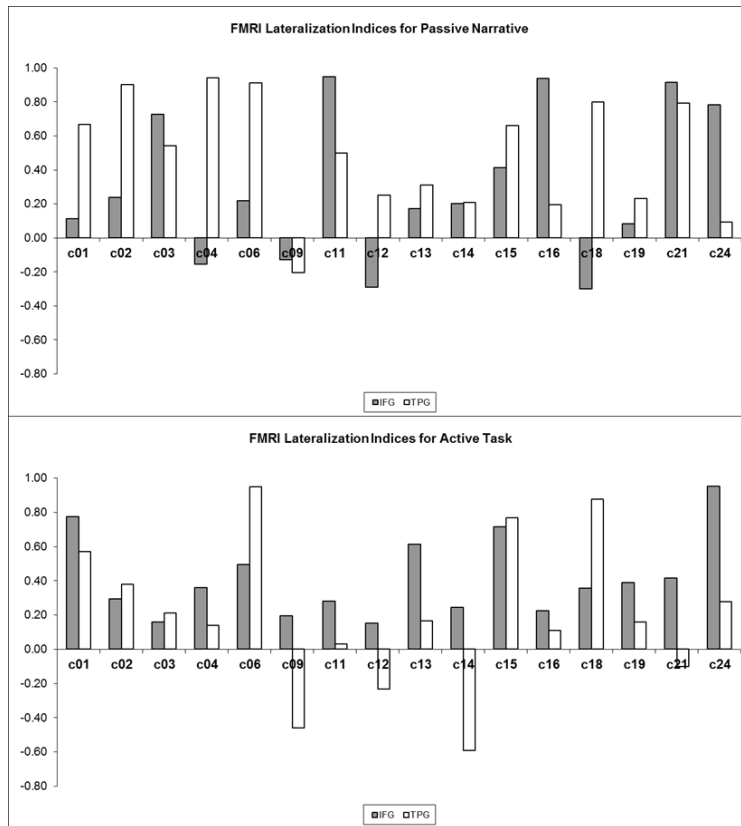


Figure 6: Control cohort lateralization indices (LI) for the inferior frontal gyrus (IFG) and temporoparietal (TPG) language regions, using activate language fMRI (top panel) and passive language fMRI (bottom panel). Positive LI values indicate left-lateralization, negative LI indicates right-lateralization, and LI values of magnitude 0.1 or less indicate bilateral activation.

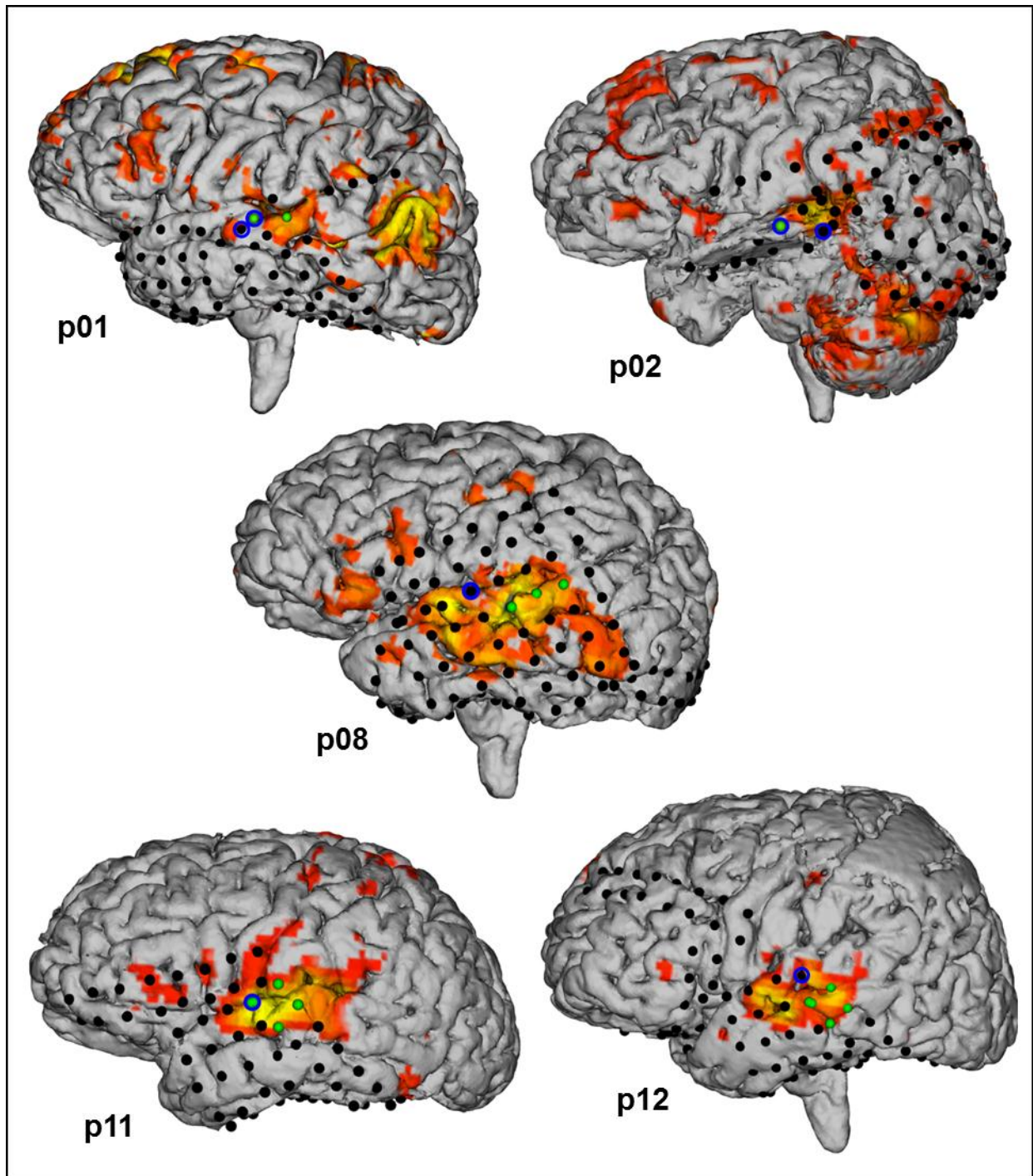


Figure 7: Three-dimensional renderings of cortical brain surfaces from the 5 participants in our patient cohort who underwent implantation of intracranial electrode strips and grids. Depicted on the cortical surfaces are the intracranial electrodes (black dots), and the cortical activation maps from passive language fMRI ($p < 0.001$ uncorrected). Note fMRI

activation patterns consistent with primary auditory activation. Note fMRI activation patterns consistent with temporoparietal receptive language processing. The electrodes of maximal frequency modulated auditory evoked responses (FMAER) are denoted by blue circles, electrode locations for essential language function by direct electrocortical stimulation (ECS) are denoted by green dots.

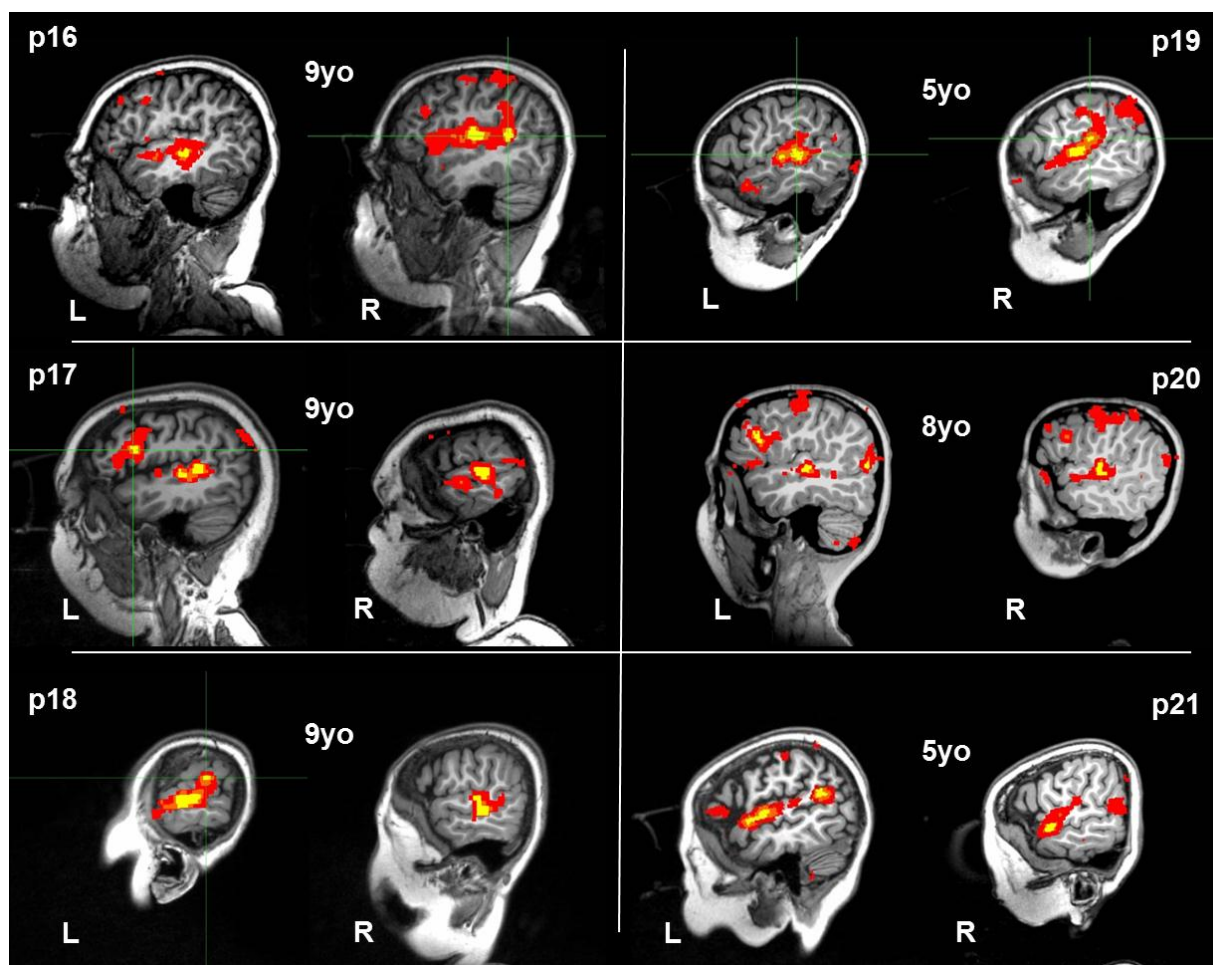


Figure 8: Passive language fMRI activation patterns recorded in patient cohort 2 ($p < 0.001$, uncorrected), made up of young patients (mean age of 7.5 years). Six of six fMRI activation patterns demonstrated bilateral primary auditory activation in the middle portion of the superior temporal gyrus consistent with typical perception of auditory narrative stimulus. Six

of six fMRI maps demonstrated lateralized activation of the temporoparietal language region consistent with typical left-dominant language-specific activation; patients p17 and p20 additionally demonstrated left-lateralized activation of the frontal language region. Patients p21 and p20 were sedated during fMRI scanning.